Ubiquitous Tracking Using Motion and Location Sensor With Application to Smartphone

Lei Wang
Department of Electrical and Computer Engineering
Missouri University of Science & Technology
Rolla, MO 65409
Email: lw3r6@mst.edu

Li Feng
Department of Mathematics Computer Science and Physics
Capital University
Columbus, OH 43209
Email: lfeng@capital.edu

Maciej Zawodniok
Department of Electrical and Computer Engineering
Missouri University of Science & Technology
Rolla, MO 65409
Email: mjzx9c@mst.edu

***Abstract*—In this paper, a cost efficient fusion scheme, Ubiquitous Tracking with Motion and Location Sensor (UTMLS), is proposed for the accurate localization and tracking in mixed GPS-friendly, GPS-challenging, and GPS-denied scenario. The proposed drift-reduction method in UTMLS addresses the cumulating error issue in the indoor tracking with the consumer grade motion sensor. The proposed hypothesis test method in UTMLS improves the tracking sensor fusion precision by detecting distorted GPS reports and intelligently switching between GPS and inertial sensor based schemes. The proposed scheme is instantiated and implemented on an Android smartphone platform. Experiments have been conducted to evaluate and validate the accuracy. Experimental results show that 1) the proposed drift-reduction method effectively suppresses the non-GPS tracking error accumulation due to the integration of acceleration noise with time 2) UTMLS realizes robust indoor/outdoor seamless tracking, preventing GPS fault estimates introduced tracking error in the conventional Kalman filtering process.**

***Keywords*—Localization; GPS; IMU; Kalman Filter; Android; Smartphone; Sensors**

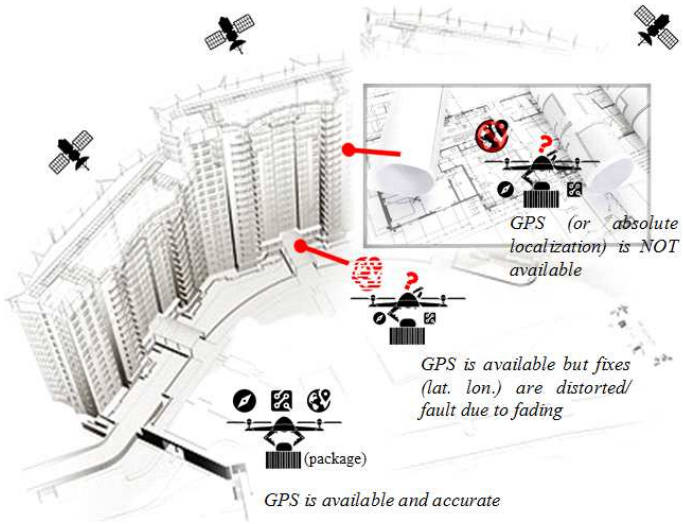

Figure 1: Motivation

I. Introduction

Location-based services (LBS) has become a key part of smart systems, including healthcare, autonomous vehicle, security, building automation, robotics, etc. Accurate localization and tracking of a mobile unit are the essential for context awareness of the applications. The global navigation satellite systems (GNSS), e.g. GPS, has long been used in mobile unit localization. In the outdoor, unobstructed environment, it provides acceptable accuracy. However, its accuracy can degrade in many situations, for example, when buildings overshadow some satellite in line-of-sight (LoS) or cause reflection (multipath fading effect), or when there is interference from a nearby device. Such a scenario with increased localization error is considered a GPS-challenging environement[1]–[3]. Moreover, since the satellite signal can be easily blocked by the buildings and ground, it is not suitable for the indoor localization which is also known as the GPS-denied environment.

Extensive research on fusion algorithms exploiting the complementary error characteristics of GPS and inertial measurement unit (IMU) have been performed for several decades [4]–[9]. However, the accurate tracking with seamless transition between GPS-friendly and GPS-challenging/fault/denied environment remains an unsolved problem. Moreover, the accuracy of an indoor (non-GPS) tracking with the low-cost motion sensor is still insufficient. Though existing step/stripe recognition and estimation methods had some success in tracking human walking, it is still challenging for robotic and wheelchair applications.

As indicated in our experimental results in Section IV-B, in the indoor and outdoor combined tracking scenario, GPS may provide erroneous position reports. This leads to undesired tracking errors. As the tracked object approaches the building, the building obstructs the signals from some satellites. Hence, the line-of-sight signals are blocked. The non-line-of-sight (NLoS) signals reflected from the surroundings distort GPS signal lock, thus inject noises in GPS pseudo-range estimation. Hence, the GPS location reports are inaccurate. When the object is entering the building, LoS signals become completely blocked, while the NLoS signals may travel through the build via reflection. As the GPS receiver makes use of these fading signals, large localization errors may occur, *which is considered as GPS fault*.

Let us consider a smart robotic package delivery application

978-1-5090-6517-2/17/$31.00 ©2017 IEEE

as shown in Fig. 1. Suppose that the autonomous robots are assigned to deliver packages door to door. Tracking and navigating the robots from warehouse to the customer building's front door have been well addressed by existing solutions (e.g. GPS). However, when the robots approach the building, the GPS location reports may become erroneous/distorted *rather than become entirely absent*. Without extra sensors (e.g., camera, sonar, lidar), it is difficult to navigate the robot entering the building. On the other hand, tracking the robots with the low-cost inertial sensor in the indoor/non-GPS environment is still challenging due to the accumulated error in displacement estimation with noise. Hence, a cost-efficient and smarter tracking and navigation approach, that can maintain sufficient indoor tracking accuracy, evaluate GPS reports, and smoothly switching between GPS and GPS-fault/denied navigation mode is desired.

In this paper, we propose a cost-effective Ubiquitous Tracking with Motion and Location Sensor (UTMLS) system which integrate the GPS and consumer grade IMU for indoor and outdoor seamless tracking. It achieves: 1) Seamless context-switching between indoor (GPS-challenging/denied) and outdoor (GPS-friendly) while maximizing the accuracy 2) the reduction of drift in the dead reckoning mode when using low-cost IMU. Moreover, the tracking accuracy is evaluated and validated by experiments with a prototype implemented on an Android smartphone platform.

For the GPS fault and challenging scenario, the proposed UTMLS detects the GPS fault through the proposed hypothesis test method which introduces the tracking robustness and improves the accuracy. The multivariate hypothesis test evaluates the GPS reading. When the reading is detected to be erroneous, the UTMLS will switch to indoor mode.

For the GPS-denied situation, existing solutions rely either on the pre-existing infrastructure, or human activity recognition (HAR) [10]–[12]. The pre-existing infrastructure augmented methods require the knowledge of the anchor nodes (e.g., WiFi access point, Bluetooth, ZigBee nodes, etc.) deployment in the building, which is difficult to obtain for security consideration in most of the scenarios. Or, it requires the time-consuming offline training (war-driving) phase to construct the radio map [13]–[15]. In contrast, in our proposed UTMLS system, infrastructure information or radio map are not required, which broadens applications and makes it more feasible for most indoor tracking scenarios.

The HAR based methods require step recognition and stride length estimation for dead reckoning. However, in the smart applications, the tracking object may be the package-delivering robots, or wheelchair, where human activities are absent in these scenarios. The proposed UTMLS makes use of only the consumer grade IMU and estimates the displacement of the object in the heading direction. A high-pass filter is introduced in the UTMLS speed estimation to conquer the drift.

The proposed system is instantiated and evaluated on an Android phone. As an ideal platform for the low-cost smart LBS, the smartphone has become more and more popular[16] . The essential GPS receiver, motion sensor(accelerometer, gyroscope), and magnetometer have already been the standard modules equipped in the mainstream smartphone. In this paper, we introduced the prototype implementation and software design of the system.

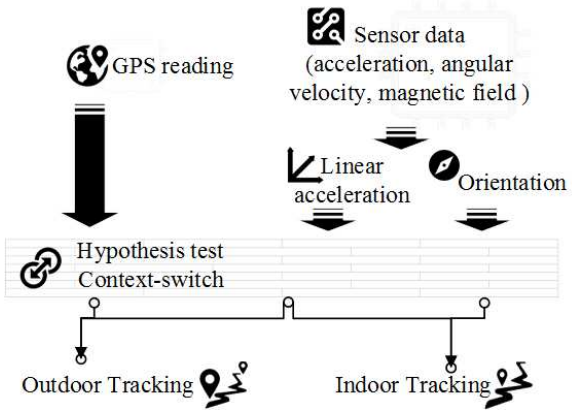

Figure 2: overview

II. Methodology

In this section, the methodology used for indoor and outdoor seamless tracking in the UTMLS system is presented.

A. Overview

Fig. 2 depicts the overall systemic strategy of sensor fusion and indoor/outdoor tracking-mode switching in the proposed UTMLS. GPS estimation of the absolute position is fed into the system. At the same time, IMU readings are fed into the indoor tracking algorithm, to calculate the non-GPS based localization information. In the next step, the *Hypothesis-test Context-switcher*, which uses kinetic model and Kalman filter, evaluates the data set. When the accuracy of GPS reports is acceptable, the system performs Kalman filtering in outdoor mode. In case that GPS fault (i.e. distorted GPS positioning) is detected, the system will switch to indoor mode. In the indoor mode, with the proposed drift-reduction method, accurate tracking (evaluated in Section IV) with the low-cost IMU is achieved.

In the following subsections, the dynamic system model and Kalman filter are briefly introduced in Section II-B. Next, the proposed hypothesis test method is introduced in Section II-C. Then, the indoor-mode tracking including the orientation and linear acceleration estimation, and velocity drift reduction is presented in Section II-D.

B. Kinetic Model and Kalman Filter

For completeness, the dynamic model and Kalman filter update law are briefly introduced here. The state space continues time representation of the kinetics can be described as [17],

$$\begin{aligned} \dot{\boldsymbol{x}} &= \boldsymbol{A}\boldsymbol{x} + \boldsymbol{B}(\boldsymbol{u} + \tilde{\boldsymbol{\sigma}}) \\ \boldsymbol{y} &= \boldsymbol{C}\boldsymbol{x} + \boldsymbol{v}. \end{aligned} \tag{1}$$

where $\boldsymbol{A}$ is the state transition matrix, $\boldsymbol{B}$ is the control input matrix, $\boldsymbol{C}$ is the measurement matrix. $\boldsymbol{u}$ represents the control

input which contains noise $\tilde{\boldsymbol{\sigma}}$. $\boldsymbol{y}$ is the measurement model with $\boldsymbol{v}$ representing the noise. $\boldsymbol{x}$ is the states in the system, and $\dot{\boldsymbol{x}}$ the derivative of it.

The kinetic model with the linear acceleration as the dynamic control input is given in Appendix A.

By discretization,

$$\boldsymbol{x}_{k+1} = \boldsymbol{F}\boldsymbol{x}_k + \boldsymbol{G}\boldsymbol{u}_k + \boldsymbol{\sigma}_k. \tag{2}$$

$$\boldsymbol{y}_k = \boldsymbol{C}\boldsymbol{x}_k + \boldsymbol{v}_k. \tag{3}$$

where $\boldsymbol{F}$ is the Taylor expansion of $e^{\boldsymbol{A}\triangle t}$ and keep the lower order terms of $\triangle t$. And, $\boldsymbol{G} = \boldsymbol{F}\int_0^{\triangle t} e^{-\boldsymbol{A}\tau}d\tau\boldsymbol{B}$. $\boldsymbol{\sigma}_k$ and $\boldsymbol{v}_k$ are the noise in the state and observation, respectively.

Assuming $\boldsymbol{\sigma}_k$ and $\boldsymbol{v}_k$ are zero mean Gaussian, the process noise covariance matrix $\boldsymbol{Q}_k = E\left[\boldsymbol{\sigma}_k\boldsymbol{\sigma}_k^T\right]$, and the measurement noise covariance matrix $\boldsymbol{\Sigma}_k = E\left[\boldsymbol{v}_k\boldsymbol{v}_k^T\right]$.

Providing the state estimation $\boldsymbol{x}_{k-1}$, we can predict the state at k, $\boldsymbol{x}_k^-$, via (2). Thus, given observation at k, the estimation of the state at k is [17], [18],

$$\boldsymbol{x}_k^+ = \boldsymbol{x}_k^- + \boldsymbol{K}_k\left(\boldsymbol{y}_k - \boldsymbol{C}\boldsymbol{x}_k^-\right) \tag{4}$$

where,

$$\begin{aligned}
&\boldsymbol{K}_k = \boldsymbol{P}_k^-\boldsymbol{C}_k^T\left(\boldsymbol{C}_k\boldsymbol{P}_k^-\boldsymbol{C}_k^T + \boldsymbol{\Sigma}_k\right)^{-1}\\
&\boldsymbol{P}_k^- = \boldsymbol{F}_{k-1}\boldsymbol{P}_{k-1}^+\boldsymbol{F}_{k-1}^T + \boldsymbol{Q}_{k-1}\\
&\boldsymbol{P}_k^+ = (\boldsymbol{I} - \boldsymbol{K}_k\boldsymbol{C}_k)\boldsymbol{P}_k^-(\boldsymbol{I} - \boldsymbol{K}_k\boldsymbol{C}_k)^T + \boldsymbol{K}_k\boldsymbol{\Sigma}_k\boldsymbol{K}_k^T.
\end{aligned} \tag{5}$$

C. Multivariate Hypothesis Test based GPS Fault Detection

In this section, Proposition 1 shows how we use covariance matrix to evaluate the accuracy of GPS location reports so as to decide whether its accuracy is sufficient or there is GPS fault. And in II-C-2, we show how to obtain the observation covariance matrix from the dynamic.

1) The Multivariate Hypothesis Test:

Let $\boldsymbol{\Sigma}$ be the covariance matrix of the GPS observation $\boldsymbol{y} = [y_1, y_2]^T$. Assume that the noise of the GPS observation on the coordinate elements, i.e., y_1, y_2, is independent. Given the ideal performance of the GPS receiver, i.e., the covariance matrix $\boldsymbol{\Sigma_0}$, in the open outdoor environment. To detect the GPS-challenging context is equivalent to compare the generalized variance $|\boldsymbol{\Sigma}|$ with $|\boldsymbol{\Sigma_0}|$.

It has been proven in [19], $\sqrt{N-1}\left(\frac{|\boldsymbol{\Sigma}|}{|\boldsymbol{\Sigma_0}|} - 1\right)$ is asymptotically distributted as Normal, $\mathcal{N}(0, 2p)$. Where N is the number of sample, $p \times p$ is the dimension of the covariance matrix.

Proposition 1 provides the criterion for the hypothesis test.

Proposition 1. *The criterion for testing the hypothesis $\boldsymbol{H}_0$: $|\boldsymbol{\Sigma}| \leqslant |\boldsymbol{\Sigma}_0|$:*

$$Z = \sqrt{\frac{N-1}{2p}}\left(\frac{|\boldsymbol{\Sigma}|}{|\boldsymbol{\Sigma}_0|} - 1\right). \tag{6}$$

The reject region (RR), $\boldsymbol{H}_1$: $|\boldsymbol{\Sigma}| > |\boldsymbol{\Sigma}_0|$, given the significant level α:

$$RR = \{|\boldsymbol{\Sigma}| : Z(|\boldsymbol{\Sigma}| \geqslant -Z_{1-\alpha})\}. \tag{7}$$

Remark 1 gives the power of the test. The power of a hypothesis test is the probability that the test correctly rejects $\boldsymbol{H}_0$ when $\boldsymbol{H}_1$ is true. A type II error occurs when $\boldsymbol{H}_0$ is false, but erroneously accepted. [20] Thus, the power of a test is found by calculate the probability of not committing a type II error. [21]

Remark 1. *The power of the test $|\boldsymbol{\Sigma}| \leqslant |\boldsymbol{\Sigma}_0|$ is,*

$$\pi(\sigma) = 1 - \boldsymbol{\phi}\left(\sqrt{\frac{(N-1)}{2p}}\left[\frac{|\boldsymbol{\Sigma}|}{\sigma}\left(1 - \sqrt{\frac{2p}{N-1}}Z_{1-\alpha}\right) - 1\right]\right). \tag{8}$$

where $\boldsymbol{\phi}(\cdot)$ is the cumulative distribution function (CDF) of the standard normal distribution.

Proof. The type II error,

$$\begin{aligned}
\boldsymbol{\beta}(\sigma) &= \mathbb{P}\left(fail\ to\ reject\ \boldsymbol{H}_0\,|\boldsymbol{H}_1\ is\ true\right)\\
&= \mathbb{P}\left(Z < -Z_{1-\alpha}\,|\,|\boldsymbol{\Sigma}_0| = \sigma\right)\\
&= \mathbb{P}\left(\sqrt{\frac{N-1}{2p}}\left(\frac{|\boldsymbol{\Sigma}|}{\sigma} - 1\right) < \sqrt{\frac{N-1}{2p}}\left[\frac{|\boldsymbol{\Sigma}|}{\sigma}\left(1 - \sqrt{\frac{2p}{N-1}}Z_{1-\alpha}\right) - 1\right]\right)\\
&= \boldsymbol{\phi}\left(\sqrt{\frac{N-1}{2p}}\left[\frac{|\boldsymbol{\Sigma}|}{\sigma}\left(1 - \sqrt{\frac{2p}{N-1}}Z_{1-\alpha}\right) - 1\right]\right)
\end{aligned}$$

Thus, the power of the test is $\pi(\sigma) = 1 - \beta(\sigma)$, which is (8). □

2) The Covariance Matrix in Observation:

The covariance matrix, $\boldsymbol{\Sigma}$, can be obtained from innovation vector,

$$\boldsymbol{i}_k = \boldsymbol{y}_k - \boldsymbol{y}_k^-. \tag{9}$$

where $\boldsymbol{y}_k^- = \boldsymbol{C}_k\boldsymbol{x}_k^-$. The covariance of the innovation is $E\left[\boldsymbol{i}_k\boldsymbol{i}_k^T\right] = \boldsymbol{C}_k E\left[(\boldsymbol{x}_k - \boldsymbol{x}_k^-)(\boldsymbol{x}_k - \boldsymbol{x}_k^-)^T\right]\boldsymbol{C}_k^T + \boldsymbol{\Sigma}_k$.

The maximum likelihood estimator of the measurement noise is [22],

$$\boldsymbol{\Sigma}_k = \boldsymbol{V}_k - \boldsymbol{C}_k\boldsymbol{P}_k^-\boldsymbol{C}_k^T. \tag{10}$$

where $\boldsymbol{V}_k = \frac{1}{N}\sum_{j=j_0}^{k}\boldsymbol{i}_j\boldsymbol{i}_j^T$. And, N is the size of the moving estimation window, $j_0 = k - N + 1$.

D. Proposed Non-GPS Tracking Scheme

In the indoor mode, the non-GPS tracking of the mobile object is calculated based on the orientation estimation and drift-reduced velocity. The proposed drift-reduction method makes accurate indoor tracking with consumer grade IMU possible.

In this section, a gradient descent algorithm is first introduced for calculating the orientation quaternion in II-D 1). Next, based on the orientation estimation, linear acceleration in the earth inertial frame is found in II-D 2). Then, in II-D 3), a drift-reduction method for the velocity estimation is presented.

1) Orientation:

The orientation of a mobile unit is the angle of the mobile body frame relative to the earth inertial frame. To determine the orientation, we integrate the gravity, angular velocity, and magnetic field measurements. They are measured by the accelerator, gyroscope, and magnetometer inside the smartphone IMU, respectively.

Let ${}^{S}_{E}\boldsymbol{q}$ be the quaternion that describes the orientation of the earth inertial frame relative to the sensor body frame.

The gyroscope measured angular velocity can be written in quaternion form as,

$$ {}^{S}\boldsymbol{\omega} = [0, \omega_x, \omega_y, \omega_z]\,. \tag{11} $$

The quaternion at time instance k can be calculated as [23],

$$ \begin{aligned} {}^{S}_{E}\dot{\boldsymbol{q}}_{\boldsymbol{\omega},k} &= \frac{1}{2}\,{}^{S}_{E}\hat{\boldsymbol{q}}_{k-1} \otimes {}^{S}\boldsymbol{\omega}_k \\ {}^{S}_{E}\boldsymbol{q}_{\boldsymbol{\omega},k} &= {}^{S}_{E}\hat{\boldsymbol{q}}_{k-1} + {}^{S}_{E}\dot{\boldsymbol{q}}_{\boldsymbol{\omega},k} \triangle t. \end{aligned} \tag{12} $$

where $\otimes$ represents the quaternion multiplication [23]. ${}^{S}_{E}\hat{\boldsymbol{q}}_{est,k-1}$ is the orientation quaternion estimation at $k-1$ epoch. And, $\hat{(\cdot)}$ represents the normalized quantity, i.e., $\|\hat{(\cdot)}\| == 1$.

Let ${}^{S}\boldsymbol{s}$ and ${}^{S}\boldsymbol{m}$ represents the acceleration and magnetic field measurement, respectively. And, the normalized reference gravity is ${}^{E}\hat{\boldsymbol{g}} = [0, 0, 0, 1]$, the earth magnetic field reference is ${}^{E}\hat{\boldsymbol{b}} = [0, b_x, 0, b_z]$. The orientation is the quaternion that minimize the function,

$$ \boldsymbol{f}({}^{S}_{E}\boldsymbol{q}) = \begin{bmatrix} {}^{S}_{E}\hat{\boldsymbol{q}}^{*} \otimes {}^{E}\hat{\boldsymbol{g}} \otimes {}^{S}_{E}\hat{\boldsymbol{q}} - {}^{S}\hat{\boldsymbol{s}} \\ {}^{S}_{E}\hat{\boldsymbol{q}}^{*} \otimes {}^{E}\hat{\boldsymbol{b}} \otimes {}^{S}_{E}\hat{\boldsymbol{q}} - {}^{S}\hat{\boldsymbol{m}} \end{bmatrix} \tag{13} $$

where $(\cdot)^*$ represents quaternion conjugate [23].

By gradient descent algorithm, the orientation quaternion,

$$ {}^{S}_{E}\hat{\boldsymbol{q}}_{\nabla,k} = {}^{S}_{E}\hat{\boldsymbol{q}}_{k-1} - \mu_k \frac{\nabla \boldsymbol{f}}{\|\nabla \boldsymbol{f}\|}. \tag{14} $$

where $\nabla \boldsymbol{f} = \left[\frac{\partial}{\partial({}^{S}_{E}\hat{\boldsymbol{q}})}\boldsymbol{f}\right]^{T} \boldsymbol{f}({}^{S}_{E}\hat{\boldsymbol{q}})$.

Thus, the orientation estimation is obtained by weighting the quaternion calculation from angular rate (12) and from gravity and magnetic field (14) [24],

$$ \begin{aligned} {}^{S}_{E}\boldsymbol{q}_k &= {}^{S}_{E}\hat{\boldsymbol{q}}_{k-1} + {}^{S}_{E}\dot{\boldsymbol{q}}_k \triangle t \\ {}^{S}_{E}\dot{\boldsymbol{q}}_k &= {}^{S}_{E}\dot{\boldsymbol{q}}_{\omega,k} - \beta \frac{\nabla \boldsymbol{f}}{\|\nabla \boldsymbol{f}\|} \end{aligned}. \tag{15} $$

2) Linear Acceleration:

The accelerometor readings are the measurements of the force along the coordinates of the sensor body frame. In ground mobile tracking application, due to the earth gravity, accelerometer reading will be nonzero even the sensor is static. The linear acceleration represents the force (without gravity) relative to the earth inertial frame, which can be estimated as,

$$ \boldsymbol{u} = {}^{S}_{E}\boldsymbol{q}\ {}^{S}\boldsymbol{s}\ {}^{S}_{E}\boldsymbol{q}^{*} - \boldsymbol{g}. \tag{16} $$

where ${}^{S}\boldsymbol{s}$ is the accelerometor reading, ${}^{S}_{E}\boldsymbol{q}$ is the orientation estimated from (15), and $\boldsymbol{g} = [0, 0, 0, g]^{T}$ ($g = 9.807 m/s^2$).

Let ${}^{S}_{E}\boldsymbol{q} = [q_1, q_2, q_3, q_4]$, the heading (the azimuth angle of the orientation) is,

$$ \psi = atan2(2q_3q_4 - 2q_1q_2,\ 2q_1^2 + 2q_4^2 - 1). \tag{17} $$

Thus, the acceleration in the heading direction can be found by the dot production of $\boldsymbol{u}$ and heading unit vector

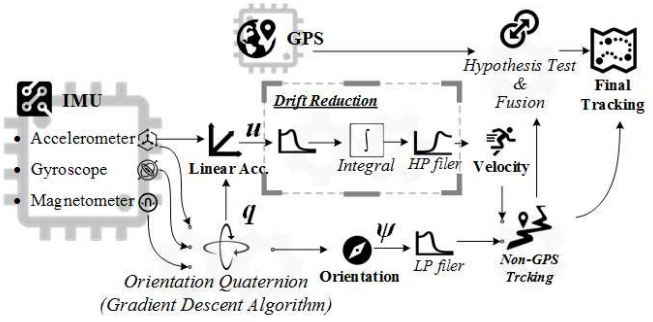

Figure 3: Sensor Data Processing Diagram

$\hat{\boldsymbol{h}} = [sin(\psi),\ cos(\psi),\ 0]^{T}$,

$$ \boldsymbol{a} = \boldsymbol{u} \cdot \hat{\boldsymbol{h}}. \tag{18} $$

3) Drift Reduction:

As indicated by the kinetic model with linear acceleration input (Appendix A), to calculate the displacement, acceleration measurement needs to be integrated first to obtain the velocity. Then, the velocity has to be integrated for the second time. Therefore, the noise in the acceleration measurements will be accumulated which result in huge drift in displacement estimation.

In the indoor mobile unit tracking, considering the limited space, we assume that the mobile object tends to stop, and there is *no strict-constant-speed* in the movement. Therefore, in our proposed UTMLS, the drift in the calculated velocity is eliminated by a high-pass filter (the "Drift Reduction" box in fig. 3).

Fig. 3 illustrates the sensor data processing procedure in our system. The accelerometer, gyroscope, (in rigid body frame) and magnetometer measured signals are first processed by quaternion based gradient descent algorithm to produce the orientation (in the earth inertial frame). Next, as shown in the "Drift Reduction" box in fig. 3, the velocity is calculated by integrating the low-pass filtered linear acceleration, and a high-pass filter for eliminating the drift. Then, with the speed and orientation, the mobile unit dead-reckoning (non-GPS tracking) is achieved. The "Hypothesis Test & Fusion" block represents the proposed hypothesis test method for evaluating the GPS accuracy. It determines whether or not that the GPS readings should be integrated with non-GPS tracking.

III. Prototype Implementation

The proposed algorithm is implemented on the Samsung Galaxy S®6 Android phone. The onboard IMU motion sensors (including the acceleration sensor, gyroscope, and geomagnetic field sensor) are accessed through Android SensorManager. The GPS latitude/longitude is periodically obtained through Android LocationManager. In our experiments, motion sensor readings are refreshed every $\triangle t = 6$ milliseconds, latitude/longitude is updated once per second. The proposed scheme including the quaternion gradient descent algorithm, kalman filter, low-pass and high-pass filters

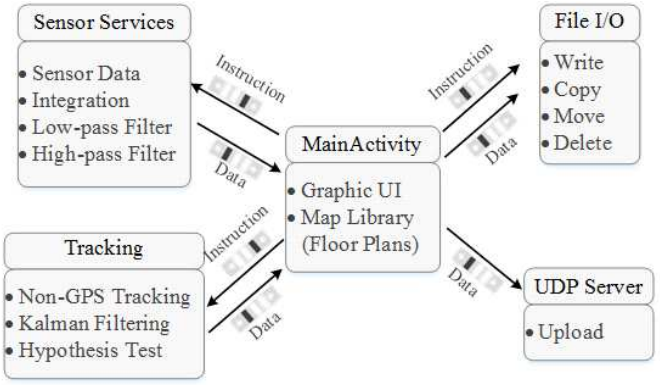

Figure 4: Software Diagram

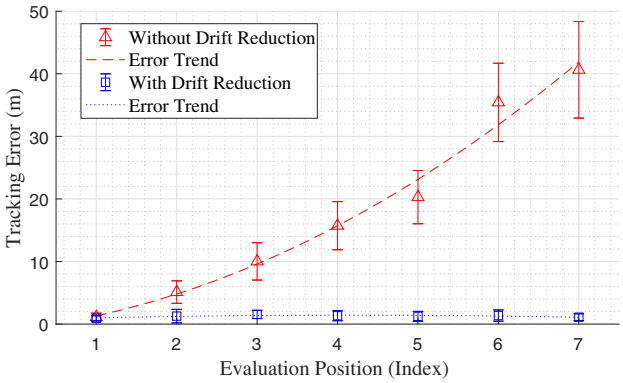

Figure 5: Indoor Tracking Error Comparison

are developed and evaluated by using the MathWorks® Matlab. Next, the Matlab code is converted into C/C++ code through MATLAB Coder. Then, the algorithm API library is built by using the Android ndk-build (native development kit) tool. Finally, C/C++ APIs are wrapped by Java Native Interface (JNI) so that they can be used in Java environment.

The software structure is illustrated in Fig. 4. The sensoring services, including the low-pass and high-pass filtering, are implemented as one Android Handler runnable object. And, the non-GPS tracking, hypothesis-test, Kalman filtering process are realized as a standalone Handler service. Besides, file I/O service is a standalone Handler thread. UDP service (for uploading data to PC Matlab evaluation program) is realized by using the Android AsyncTask. Handler threads exchange information with MainActivity through Android MessageQueue.

IV. Experimental Results

In the Samsung Galaxy S®6, a 6-axis MotionTracking device, InvenSense® MPU-6500™, provides a 0.3mg noising accelerometer and a $\pm 5°/s$ zero-rate-output $0.1°/s$ noising gyroscope [25], [26].

For the evaluation of the proposed system, two experiments are conducted. First, an indoor experiment is first implemented to evaluate the non-GPS tracking accuracy. In the second experiment, an experimental path is chosen to traverse the building. The tracking error of the proposed hypothesis test based fusion method is compared with conventional Kalman filtering result.

The actual/reference path that the experimenter followed is shown in Appendix B Fig. 10a, Fig. 10b. The indoor experiment is conducted on the 3rd floor of engineering research building (ERL), Missouri University of Science & Technology. While, for the indoor-outdoor complex scenario, the experiment is implemented on the 1st floor inside, and sidewalk outside (near) the ERL building.

A. Non-GPS Tracking

In our indoor tracking experiment, twenty trials are conducted. At the same time, the tracking results by using the conventional non-drift-reduction method are recorded for comparison.

In Fig. 5, the tracking errors with and without the proposed drift reduction are compared. The x-axis of the figure represents the index of *evaluation positions* shown in Fig.10a (Appendix B). For the purpose of comparison, tracking errors along the evaluation positions are fitted with second-order polynomial by using the linear regression. From Fig.5 we found that without drift reduction, the tracking error increases along with the moving distance (/time). In contrast, the error is maintained at a constant level when drift reduction is applied. Therefore, the proposed drift reduction method effectively suppressed the accumulated error in the tracking.

The tracking errors and error standard deviations at each evaluating position are shown in Table I. On average, the error of the drift-reduction based tracking is 1.027 *m*. (Tracking

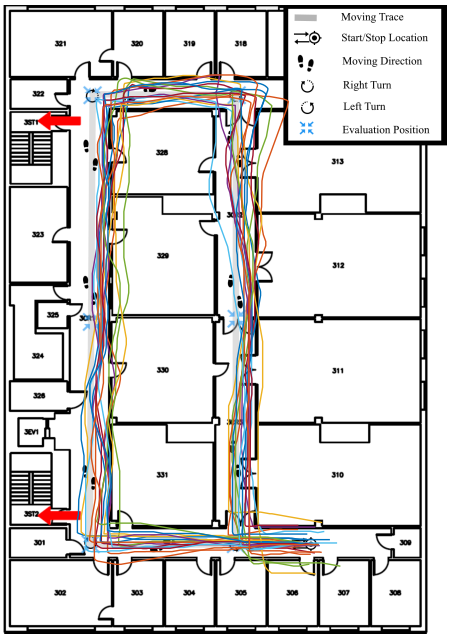

Figure 6: Proposed Non-GPS Tracking Results

Table I: Tracking Error Comparison

Pos. Idx.[a]	D.R.[b] (m)		w/o D.R[c] (m)		Imprv.[d]
	err.	std. dev.	err.	std. dev.	
1	0.930	0.402	1.132	0.618	18%
2	1.277	1.079	5.120	1.796	75%
3	1.544	0.653	10.022	2.983	85%
4	1.339	0.809	15.728	3.850	91%
5	1.236	0.799	20.29	4.257	94%
6	1.366	0.903	35.434	6.257	96%
7	1.107	0.542	40.64	7.715	97%

[a] Position Index (Appendix B Fig.10a)
[b] Drift Reduction
[c] Without Drift Reduction
[d] Improvement of **D.R.** over **w/o D.R.**

results of the twenty trials are shown in Fig. 6 for reference.) While, without the proposed drift reduction, the averaged tracking error is accumulated with acceleration noise.

The proposed non-GPS tracking method effectively reduced the drift in the velocity estimation, hence the overall tracking accuracy is improved.

B. UTMLS

The tracking error of the proposed UTMLS and conventional Kalman filtering results are compared in Fig.7. The tracking "Error Trend" in the figure are the linear regression result of fitting the error data with the second-order polynomial. The "Error Trend" of the Kalman filtering based tracking shows an error divergence along with the evaluation positions (distance), whereas the UTMLS based one prevents the error deviation. This can be interpreted by Fig.8 which is one field trial instance in our experiment. As the tracked object is traveling into the building, since the GPS receiver makes use of the fading signal estimating the pseudo-range, erroneous position reports are provided. Therefore, in Fig.8, the "GPS Trace" diverges from the actual moving trajectory and "GPS error" gets large. Hence, the conventional Kalman filtering result is distorted by this GPS fault.

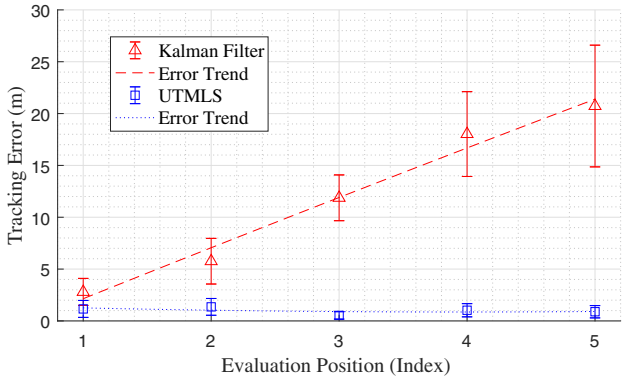

Figure 7: Tracking Error Comparison between UTMLS and Kalman Filtering

Table II shows the tracking error of the proposed UTMLS and Kalman Filtering results. In the table, the UTMLS has less error comparing to the conventional Kalman filtering result at each evaluating position (Appendix B Fig.10b). This is due to the fact that, when the tracked object enters the building, the UTMLS effectively detects the GPS fault and switches the tracking mode. The erroneous GPS reports are prevented in the sensor fusion algorithm.

Table II: Tracking Error in GPS Challenging/Fault Scenario

Pos. Idx.[a]	UTMLS (m)		Kalman (m)		Imprv.[b]
	err.	std. dev.	err.	std. dev.	
1	1.1582	0.81751	2.799	1.3034	59%
2	1.3558	0.8102	5.761	2.2013	76%
3	0.93447	0.35703	11.88	2.2081	92%
4	1.0309	0.63664	18.02	4.0904	94%
5	0.88671	0.59365	20.73	5.8701	96%

[a] Position Index (Appendix B Fig.10b)
[b] Improvement of *UTMLS* over *Kalman Filtering*

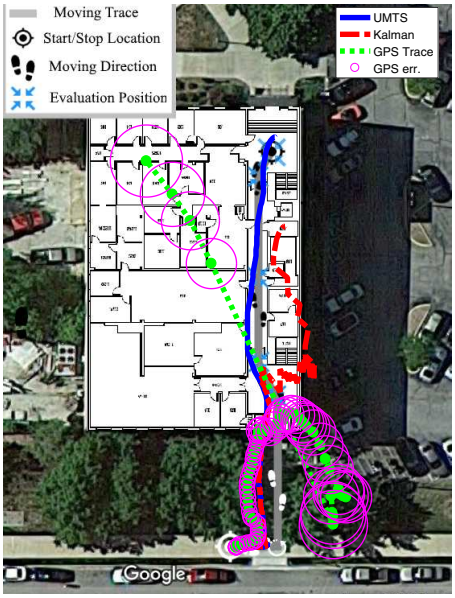

Figure 8: Comparison of UTMLS, Kalman Filtering, and GPS Fixed &Accuracy

V. Conclusion and Future Works

The proposed UTMLS system is successfully evaluated and validated by experiments with the prototype implementation on the smartphone platform. Experimental results show that the proposed non-GPS tracking method effectively suppressed the drift in consumer grade IMU based navigation. The average accuracy of $1^{-}m$ error is achieved. The proposed hypothesis test method effectively detected the GPS fault. Overall, the UTMLS system achieves accurate mobile object tracking in mixed GPS-friendly, GPS-challenging, and GPS-denied scenario. It maintains $1^{-}m$ accuracy throughout the conducted experiments in the complex indoor & outdoor environments, which is $90^{+}\%$ accurate than conventional Kalman filtering.

The future work should include developing a smarter context-aware fusion of the different location information. For example, to detect and correct when compass readings are skewed by a large metallic object.

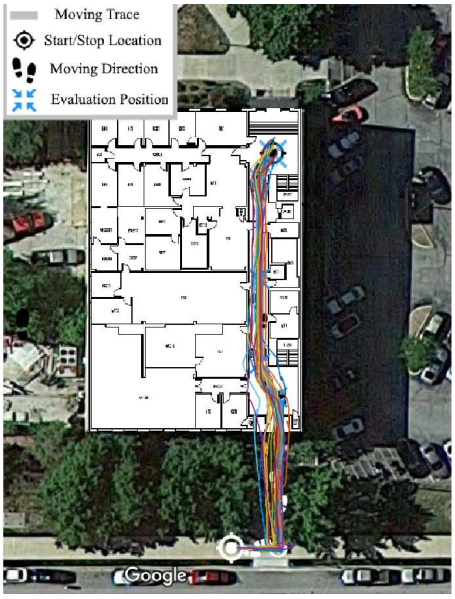

Figure 9: Proposed UTMLS Tracking Results

APPENDIX A
KINETIC MODEL (LINEAR ACCELERATION INPUT)

Let the state of the kinetic model encapsulate the displacement and velocity along the north east coordinates in the earth inertial frame,

$$\boldsymbol{x} = [x_1, v_1, x_2, v_2]^T. \tag{19}$$

where $[x_1, x_2]$ represents the displacements of the mobile unit along north and east directions, and $[v_1, v_2]$ is the speeds. And, the linear acceleration as the control input, i.e., $\boldsymbol{u} = [a_1, a_2]^T$.

The dynamic model matrices are,

$$\begin{aligned} \boldsymbol{A} &= \begin{bmatrix} 0 & 1 & 0 & 0 \\ 0 & 0 & 0 & 0 \\ 0 & 0 & 0 & 1 \\ 0 & 0 & 0 & 0 \end{bmatrix}, \ \boldsymbol{B} = \begin{bmatrix} 0 & 0 \\ 1 & 0 \\ 0 & 0 \\ 0 & 1 \end{bmatrix}, \\ \boldsymbol{F} &= \begin{bmatrix} 1 & \triangle t & 0 & 0 \\ 0 & 1 & 0 & 0 \\ 0 & 0 & 1 & \triangle t \\ 0 & 0 & 0 & 1 \end{bmatrix}, \ \boldsymbol{G} = \begin{bmatrix} \frac{(\triangle t)^2}{2!} & 0 \\ \triangle t & 0 \\ 0 & \frac{(\triangle t)^2}{2!} \\ 0 & \triangle t \end{bmatrix}. \end{aligned} \tag{20}$$

APPENDIX B
MOVING PATH IN THE EXPERIMENTS

Fig. 10a and Fig. 10b show the paths along which the experiments are conducted.

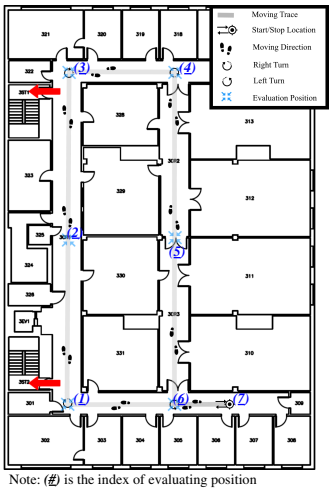

Note: (#) is the index of evaluating position

(a) Indoor Moving Path

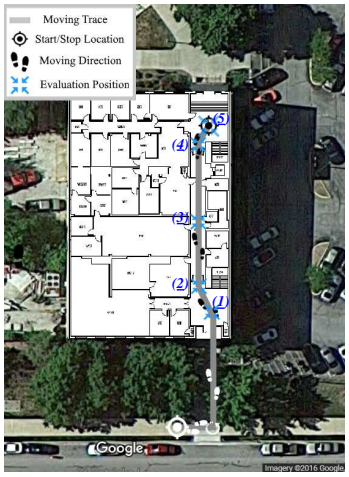

Note: (#) is the index of evaluating position

(b) Indoor/Outdoor Path

Figure 10: outdoor/Indoor Moving Path

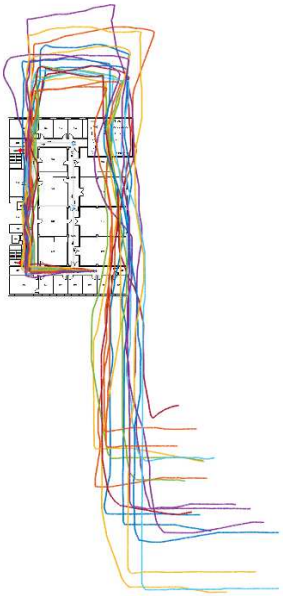

Figure 11: Without Drift Reduction

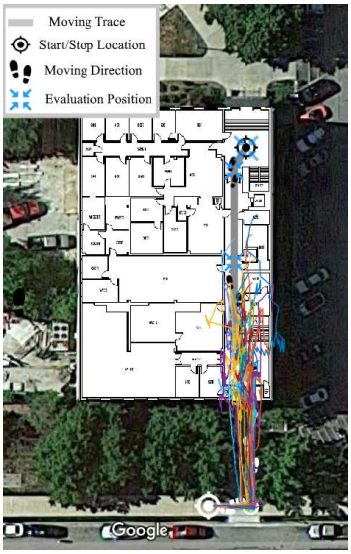

Figure 12: Kalman Filtering Results

REFERENCES

[1] P. Misra and P. Enge, *Global positioning system: signals, measurements, and performance*. Ganga-Jamuna Press, 2006.

[2] B. Lubbers, S. Mildner, P. Oonincx, and A. Scheele, "A study on the accuracy of GPS positioning during jamming," in *2015 International Association of Institutes of Navigation World Congress (IAIN)*, Oct. 2015, pp. 1–6.

[3] M. L. Psiaki, T. E. Humphreys, and B. Stauffer, "Attackers can spoof navigation signals without our knowledge. Here's how to fight back GPS lies," *IEEE Spectrum*, vol. 53, no. 8, pp. 26–53, Aug. 2016.

[4] W. Yan, L. Wang, Y. Jin, and G. Shi, "High accuracy Navigation System using GPS and INS system integration strategy," in *2016 IEEE International Conference on Cyber Technology in Automation, Control, and Intelligent Systems (CYBER)*, Jun. 2016, pp. 365–369.

[5] M. Zhong, J. Guo, and Q. Cao, "On Designing PMI Kalman Filter for INS/GPS Integrated Systems With Unknown Sensor Errors," *IEEE Sensors Journal*, vol. 15, no. 1, pp. 535–544, Jan. 2015.

[6] L. Bowen and Y. Danya, "Calculation of vehicle real-time position overcoming the GPS positioning latency with MEMS INS," in *Proceedings of 2014 IEEE International Conference on Service Operations and Logistics, and Informatics*, Oct. 2014, pp. 248–254.

[7] A. Noureldin, A. El-Shafie, and M. Bayoumi, "GPS/INS integration utilizing dynamic neural networks for vehicular navigation," *Information Fusion*, vol. 12, no. 1, pp. 48–57, Jan. 2011. [Online]. Available: https://www.sciencedirect.com/science/article/pii/S1566253510000175

[8] Mohammed Olama, Charalambos Charalambous, Ioannis Papageorgiou, Seddik Djouadi, and Teja Kuruganti, *Position and Velocity Tracking in Cellular Networks Using the Kalman Filter*. INTECH Open Access Publisher, 2009, oCLC: 884025728.

[9] J. L. Crassidis, "Sigma-point Kalman filtering for integrated GPS and inertial navigation," *IEEE Transactions on Aerospace and Electronic Systems*, vol. 42, no. 2, pp. 750–756, 2006. [Online]. Available: http://ieeexplore.ieee.org/abstract/document/1642588/

[10] M. Alzantot and M. Youssef, "UPTIME: Ubiquitous pedestrian tracking using mobile phones," in *2012 IEEE Wireless Communications and Networking Conference (WCNC)*, Apr. 2012, pp. 3204–3209.

[11] M. Youssef, M. A. Yosef, and M. El-Derini, "GAC: energy-efficient hybrid GPS-accelerometer-compass GSM localization," in *Global Telecommunications Conference (GLOBECOM 2010), 2010 IEEE*. IEEE, 2010, pp. 1–5.

[12] I. Constandache, R. R. Choudhury, and I. Rhee, "Towards mobile phone localization without war-driving," in *Infocom, 2010 proceedings ieee*. IEEE, 2010, pp. 1–9.

[13] I. Haque and C. Assi, "Profiling-Based Indoor Localization Schemes," *IEEE Systems Journal*, vol. 9, no. 1, pp. 76–85, Mar. 2015.

[14] B. Wang, S. Zhou, W. Liu, and Y. Mo, "Indoor Localization Based on Curve Fitting and Location Search Using Received Signal Strength," *IEEE Transactions on Industrial Electronics*, vol. 62, no. 1, pp. 572–582, Jan. 2015.

[15] H. Laitinen, J. Lahteenmaki, and T. Nordstrom, "Database correlation method for gsm location," in *Vehicular Technology Conference, 2001. VTC 2001 Spring. IEEE VTS 53rd*, vol. 4. IEEE, 2001, pp. 2504–2508.

[16] "Ericsson Mobility Report." [Online]. Available: https://www.ericsson.com/res/docs/2016/ericsson-mobility-report-2016.pdf

[17] D. Simon, *Optimal State Estimation: Kalman, H Infinity, and Nonlinear Approaches*. Wiley-Interscience, 2006.

[18] R. E. Kalman, "A new approach to linear filtering and prediction problems," *Journal of basic Engineering*, vol. 82, no. 1, pp. 35–45, 1960.

[19] T. W. Anderson, Ed., *An Introduction to Multivariate Statistical Analysis*. Wiley, 1984.

[20] L. J. Bain and M. Engelhardt, *Introduction to probability and mathematical statistics*. Duxbury Press Belmont, CA, 1992, vol. 4.

[21] P. D. Ellis, *The Essential Guide to Effect Sizes: Statistical Power, Meta-Analysis, and the Interpretation of Research Results*. Cambridge University Press, Jul. 2010, google-Books-ID: 5obZnfK5pbsC.

[22] A. H. Mohamed and K. P. Schwarz, "Adaptive Kalman Filtering for INS/GPS," *Journal of Geodesy*, vol. 73, no. 4, pp. 193–203, May 1999. [Online]. Available: http://link.springer.com/article/10.1007/s001900050236

[23] J. B. Kuipers, *Quaternions and Rotation Sequences: A Primer with Applications to Orbits, Aerospace, and Virtual Reality*. Princeton University Press, 2002.

[24] S. O. Madgwick, A. J. Harrison, and R. Vaidyanathan, "Estimation of IMU and MARG orientation using a gradient descent algorithm," in *2011 IEEE International Conference on Rehabilitation Robotics*. IEEE, 2011, pp. 1–7.

[25] "MPU-6500 Product Specification Revision 1.1." [Online]. Available: http://www.glynstore.com/invensense-mpu-6500-6-axis-gyroscope-accelerometer-sensor-ic/

[26] "Inside the Samsung Galaxy S6 | Chipworks." [Online]. Available: https://www.chipworks.com/about-chipworks/overview/blog/inside-the-samsung-galaxy-s6